Proceedings of the Pakistan Academy of Sciences:
A. Physical and Computational Sciences 53 (2): 163–176 (2016)

ISSN: 0377 - 2969 (print), 2306 - 1448 (online)

Pakistan Academy of Sciences

Research Article

Design, Modeling and Simulation of Six Degree of Freedom Machining Bed

Muhammad F. Shah*, Zareena Kausar, and Faizan K. Durrani

Department of Mechatronics Engineering, Air University,
Islamabad, Pakistan

Abstract: Machining is a process in which a raw material is cut into desired shape and size after various material removal processes. As application becomes more complex and size shrinks, machines need to be designed to meet the desired precision and accuracy. To date researchers and practitioners generate 6 degree of freedom for the tool which affects the accuracy and precision of machining. In this paper it is proposed to produce the desired degrees of freedom from the bed replacing a machine bed with a parallel manipulator having six legs of variable lengths. This will give work piece a 6 DOF motion. The paper presents design for the proposed machine bed, kinematic model for the machine bed and dynamics model of the linear actuator. The linear actuator is used to change the lengths of legs. Each leg will consist of a linear actuator. The physical model of the proposed bed is generated in Solid Works, software used to model the engineering systems. Six degree of freedom motion for the proposed machining bed is simulated in the Solid Works. Results which verify that the proposed design is capable to produce motion in six directions in space are presented. Results in tabular form are presented which verify kinematic modelling of the platform while the dynamics model of linear actuator is verified through MATLAB® Simulations. All simulation results support the hypothesis that 6 DOF may be produced by a machining bed.

Keywords: Machining, Stewart platform, DOF, linear actuator; machine bed

1. INTRODUCTION

Machining is a term used to describe the removal of material from a work piece to get the desired shape. Machining process is usually categorised as drilling, milling and turning [1]. Machining is necessary where constricted tolerances on dimensions and finishing are essential. Present-day spindle technologies used for material removal give very high rotational speed and power ratings so this enables the material to remove very quickly. Unfortunately, the performance envelope for conventional machine structures limits the application of higher performance spindles. The high speed tools are also vulnerable to external and internal vibrations. In the presence of vibrations the cuts made and the parts created will be dimensionally inaccurate and imprecise. A solution of these problems is to restrict the tool motion in a single dimension and instead give 6-DOF to the machine bed. For this purpose a parallel robotic mechanism is proposed [2] to be used as a bed for micro machining. This research also proposes for machining to replace the existing beds with a 6-DOF manipulator.

There are different types of manipulators serial as well as parallel. For tackling this problem we proposed a parallel manipulator as it offers high stiffness, high dynamics and less position accuracy errors [3]. Due to their high accuracy, high control and high load capacity parallel manipulators have received a lot of attention from industries and robotics community as well [4]. However, parallel manipulators have some drawbacks of difficult forward kinematics and relatively small workspace. Generally, forward kinematics of a parallel manipulator is difficult to solve. Liu et al. [5] proposed a numerical algorithm

Received, December 2015; Accepted, May 2016
*Corresponding Author: Muhammad Faizan Shah; Email: shahfaizan250@gmail.com

which provided the kinematic solutions based on a set of three nonlinear simultaneous equations. On the other hand, dynamics of a parallel manipulator, which is very important to develop a controller, tends to be complicated. Most studies on dynamics have been performed based on the Lagrangian formulation [6], the Newton–Euler formulation [7] and the principle of virtual work [8]. These dynamic equations were accurate by including actuating legs having closed-loop connections to each other in its formulation, but computation of the dynamics was very time-consuming. Also in real-time calculation was not easy to achieve in the control system. Fichter [9] reported simulation-based control analysis but the ways of dealing with computational burden in real-time implementation were not mentioned. In case where the platform was used as a tool holder, an accurate modelling of dynamics, including legs, is required for control performance [10].

Proposed parallel manipulator is one of the types of Stewart platform in which the tool is fixed and all the motions are generated by bed [11]. With the flexibility of a Parallel Mechanism, tool may not need to be set again and again, whereas, the conventional robots need adjustments to these stations often require shutting down the entire line to reset tool for a different part to be done. Many manufacturers have developed commercial machining centres based by using Stewart Platform architecture but the literature [12, 13] lacks research in this area. The proposed 6 DOF include three linear movements (lateral, longitudinal and vertical), and the three rotations pitch, roll, and yaw.

The mechanism of the bed of the platform is presented in section 2. Solid works model to explain the motion of the bed is presented and its Kinematics is explained in the form of inverse kinematics in the following section while Dynamics model of linear actuator is presented in section 4. The simulation results which verify the proposed design and model are presented in section 5.

2. MECHANISM DESIGN AND ANALYSIS

The mechanism to produce six degrees of freedom for the work piece is proposed to be from the family of Stewart platforms which give inventive solutions to complex motion applications requiring high load capacity and accuracy in up to six independent axes [14].There are several configurations of the 6 DOF parallel manipulators depending upon the distribution of six points on the base and top plates of the platform. The configuration proposed for the machining bed is 3-6 configuration. In this configuration the base plate is divided into three sections. At each section two legs are joined to the plate at same or closest points while the top plate has six sections and each section has joint of one leg.

A schematic of the proposed mechanism for machining bed is shown in Fig. 1. This consists of a movable top plate which is connected with a fixed base plate with six independent linear actuators [15]. These linear actuators act as a kinematic chain between upper rigid plate and lower fixed plate of the platform. Linear actuators at the base plate are attached through universal joints each giving motion in 2 DOF whereas linear actuators are connected with the help of ball and socket joint with the top moving plate. Each ball and socket joint give motion in 3 axes. Anything placed on the top plate will be able to move in six DOF with the help of these linear actuators as the leg lengths of these actuators is variable.

The reachable workspace is the collection of all points $\{x\ y\ z\}^T$ that can be reached by the manipulator in at least one orientation. A subset of reachable workspace is dexterous workspace that is the volume of space that can be reached by the parallel manipulator in all orientations consequently. Dexterous workspace is null for the proposed parallel manipulator machining bed, as this cannot reach all orientations at any position in the reachable workspace. The workspace of the machining bed is defined based on assumptions that there is no actuator constraint, leg interference and singularities.

3. KINEMATICMODELINGOF THE MACHINING BED

Kinematic analysis of the machining bed is considered without regard of the forces. In kinematic analysis velocity and position are analysed for the manipulator [16]. There are two categories of kinematic analysis: Forward and inverse. In this research we propose inverse kinematics for the manipulator as the final position of the end effector is known to us and we owe to find the orientation of the legs to reach the

end point. The end point is assumed to be the final position of the centre of the top moving plate of the bed. The solution obtained is unique, and can be simply determined. Symbols used in modelling of the system are described in Table 1. Forward Kinematics is not recommended for this study as forward kinematics gives us the final position of the end effector, whereas, we need to find out the displacement of actuators.

Table 1. Description of symbols / nomenclature used.

Symbol	Description
V_b	Back Electromotive force (emf)
$\omega_m(t)$	Angular velocity of motor
k_b	Back emf constant
$i_a(t)$	Armature current
$e_a(t)$	Applied armature voltage
$T_m(s)$	Torque developed by the motor
K_t	Motor Torque Constant
D_m	Equivalent viscous damping of motor
J_m	Equivalent inertia of motor
l	Lead of screw of linear actuator
$\|I_i\|$	Length of each linear actuator
T	Translation Vector
P_I	Vector defining the coordinates of the anchor point with respect to the Platform
B_i	Vector defining the coordinates of the lower anchor point of the base of the platform

The machining bed's two plates are connected by six variable length legs. The reference framework is considered to be at the base plate [17]. In Fig. 2 schematic view of *i*th leg of parallel manipulator machining bed is shown, where T is the translation vector and Pi is the vector which defines upper anchor point with respect to the platform frame work. Translation vector T and P_i are added with each other by head to tail rule where vector G_i is the resultant vector. Vector l_i represents length of a linear actuator and B_i is the vector that defines the coordinates of the lower anchor point. These two vectors are also added by head to tail rule and the resultant vector is G_i.

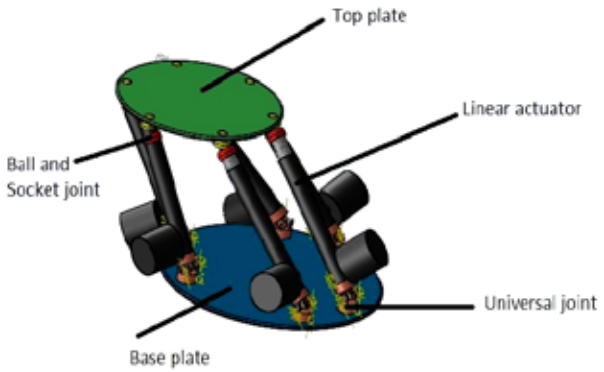

Fig. 1. Schematic diagram of the parallel manipulator bed.

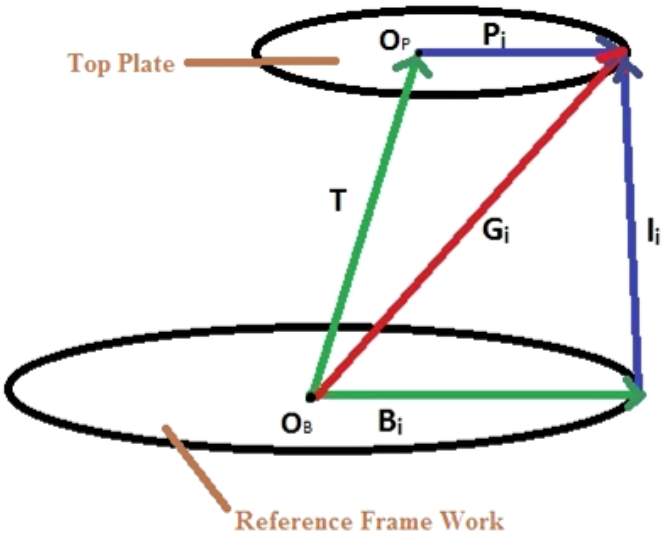

Fig. 2. Schematic view of the i_{th} leg of the parallel manipulator machining bed.

From Fig. 2, using the geometric relations and vector addition the equations (1-5) are established.

$$\overrightarrow{G_i} = \vec{T} + \vec{P_i} \tag{1}$$

$$\overrightarrow{G_i} = \vec{T} + {}^{P}_{B}R\vec{P_i} \tag{2}$$

$$\overrightarrow{G_i} = \overrightarrow{I_i} + \overrightarrow{B_i} \tag{3}$$

$$\overrightarrow{I_i} + \overrightarrow{B_i} = \vec{T} + {}^{P}_{B}R\vec{P_i} \tag{4}$$

$$\overrightarrow{I_i} = \vec{T} + {}^{P}_{B}R\vec{P_i} - \overrightarrow{B_i} \tag{5}$$

where,

$$Length\ of\ actuator = |I_i| \tag{6}$$

And *i* vary from 1 to 6.

Moreover, T is the translation vector, giving the positional linear displacement of the origin of the moving plate frame with respect to the base reference framework, and $\mathbf{P}_i$ is the vector defining the coordinates of the anchor point with respect to the moving plate framework and $\mathbf{B}_i$ is the vector defining the coordinates of the lower anchor point. These 6 equations give the lengths of the six legs to achieve the desired position of the platform.

In Fig. 3 and 4, distribution of the joint positions is given. The top moving plate is divided into six equally distant positions. Therefore, angle between each joint position is 60 degrees. On the bottom stationary plate the circular plate is divided into three parts: 120 degrees apart from each other. In each parttwo joints (say B_1 and B_2) are placed which are 35 degrees away from each other.

From Fig. 3, the equations (7-12) are established for positions of joints at top moving plate:

$$P_1 = [r \quad 0 \quad 0] \tag{7}$$

$$P_2 = [rcos60 \quad rsin60 \quad 0] \tag{8}$$

$$P_3 = [-rcos60 \quad rsin60 \quad 0] \tag{9}$$

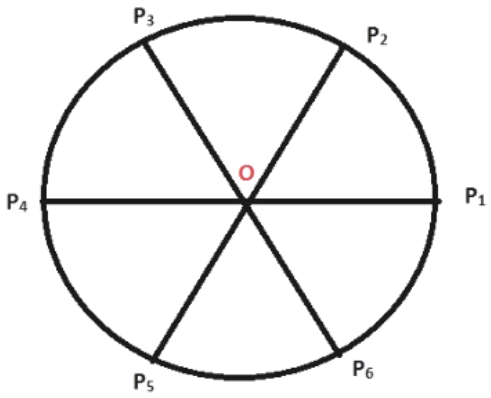

Fig. 3. Angle distribution for positioning of joints on top moving plate.

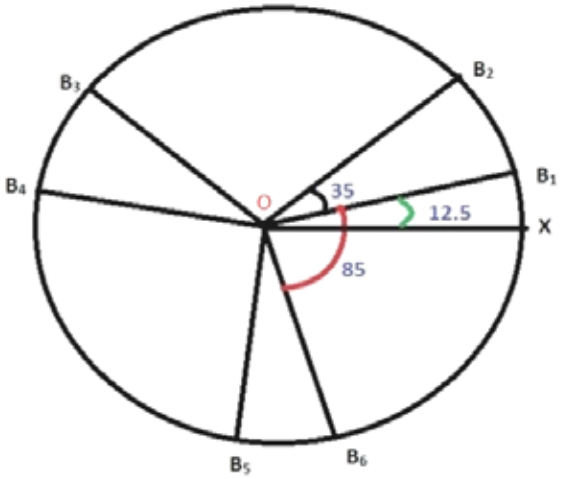

Fig. 4. Angle distribution for positioning of joints on bottom stationary plate.

$$P_4 = [-r \quad 0 \quad 0] \tag{10}$$

$$P_5 = [-rcos60 \quad -rsin60 \quad 0] \tag{11}$$

$$P_6 = [rcos60 \quad -rsin60 \quad 0] \tag{12}$$

Where *r* is the radius of the top moving plate.

Similarly from Fig. 4, the equations (13-18) are established for positions on stationary base plate:

$$B_1 = [Rcos12.5 \quad Rsin12.5 \quad 0] \tag{13}$$

$$B_2 = [Rcos47.5 \quad Rsin47.5 \quad 0] \tag{14}$$

$$B_3 = [-Rcos47.5 \quad Rsin47.5 \quad 0] \tag{15}$$

$$B_4 = [-Rcos12.5 \quad Rsin12.5 \quad 0] \tag{16}$$

$$B_5 = [-Rcos17.5 \quad -Rsin17.5 \quad 0] \tag{17}$$

$$B_6 = [Rcos17.5 \quad -Rsin17.5 \quad 0] \tag{18}$$

Where, R is the radius of the bottom stationary plate.

The rotation matrix for rotation from O_B to O_P is calculated as given in (19).

$$\begin{aligned}
&{}^{P}_{B}R = R_Z(\psi) + R_Y(\theta) + R_X(\varphi) \\
&= \begin{pmatrix} \cos(\psi) & -\sin(\psi) & 0 \\ \sin(\psi) & \cos(\psi) & 0 \\ 0 & 0 & 1 \end{pmatrix} . \begin{pmatrix} \cos(\theta) & 0 & -\sin(\theta) \\ 0 & 1 & 0 \\ -\sin(\theta) & 0 & \cos(\theta) \end{pmatrix} . \begin{pmatrix} 1 & 0 & 0 \\ 0 & \cos(\varphi) & -\sin(\varphi) \\ 0 & sin(\varphi) & \cos(\varphi) \end{pmatrix} \\
&= \begin{pmatrix} \cos(\psi)\cos(\theta) & -\sin(\psi) & \cos(\psi)\sin(\theta) \\ \sin(\psi)\cos(\theta) & \cos(\psi) & \sin(\psi)\sin(\theta) \\ -\sin(\theta) & 0 & \cos(\theta) \end{pmatrix} . \begin{pmatrix} 1 & 0 & 0 \\ 0 & \cos(\varphi) & -\sin(\varphi) \\ 0 & sin(\varphi) & \cos(\varphi) \end{pmatrix} \\
&= \begin{pmatrix} \cos(\psi)\cos(\theta) & -\sin(\psi)\cos(\varphi) + \cos(\psi)\sin(\theta)\sin(\varphi) & \sin(\psi)\sin(\varphi) + \cos(\psi)\sin(\theta)\cos(\varphi) \\ \sin(\psi)\cos(\theta) & \cos(\psi)\cos(\varphi) + \sin(\psi)\sin(\varphi)\sin(\theta) & -\cos(\psi)\sin(\varphi) + \sin(\psi)\sin(\theta)\cos(\varphi) \\ -\sin(\theta) & \cos(\theta)\sin(\varphi) & \cos(\theta)\cos(\varphi) \end{pmatrix}
\end{aligned} \tag{19}$$

Where, ψ, θ and Φ are angles of rotation about X, Y and Z axis respectively.

In conclusion, the leg length of each leg of the bed is calculated using (5) knowing the orientation of center of the top plate of the bed (where work piece needs to be moved). From known orientation T is calculated and value of rotation matrix from (19), value of Bi from (13-18) and Pi from (7-12) are calculated and substituted in (5).

4. DYNAMICS MODELLING OF LINEAR ACTUATOR

A linear actuator is an actuator that creates motion in a straight line, in contrast to the circular motion of a conventional electric motor. From Fig. 5 it can be seen that current carrying armature is rotating in a magnetic field, its voltage is proportional to speed [18]. Thus

$$v_b(t) = k_b \frac{d\theta_m(t)}{dt} \tag{20}$$

Where,

$v_b(t)$is back electromotive force ,k_b is constant of proportionality (back emf constant) and $\frac{d\theta_m(t)}{dt} = \omega_m(t)$ is the angular velocity of the motor.

The relationship between the armature current $i_a(t)$, the applied armature voltage $e_a(t)$ and the back emf $v_b(t)$ is given by writing equation (21) for a loop transformed armature circuit in Laplace form

$$R_a I_a(s) + L_a(s) I_a(s) + V_b(s) = E_a(s) \tag{21}$$

Torque developed by the motor is proportional to the armature current

$$T_m(s) = K_t I_a(s) \tag{22}$$

Where

$T_m(s)$ is Torque developed by the motor and $K_t = \text{Motor torque constant}$ which depends on the motor and magnetic field constants. Fig.6 shows a typical equivalent mechanical loading on a motor. J_m is the equivalent inertia. D_m is the equivalent viscous damping at the armature and includes both the armature viscous damping . From Fig.6:

$$T_m(s) = (J_m s^2 + D_m s)\theta_m(s) \tag{23}$$

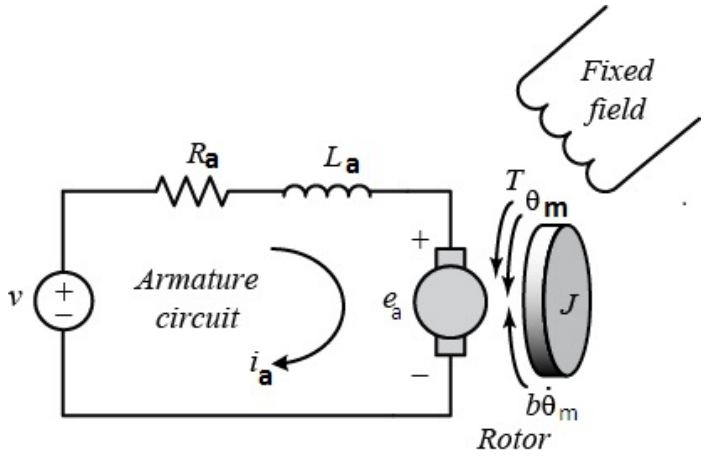

Fig. 5. Schematic diagram of the DC motor.

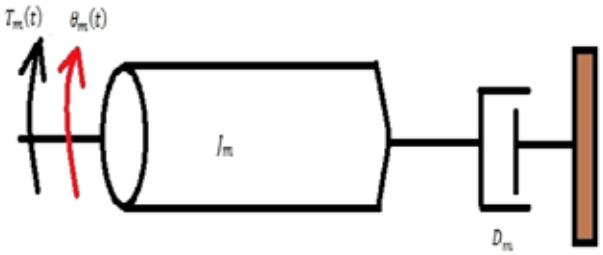

Fig. 6. Representative equivalent mechanical load in a motor.

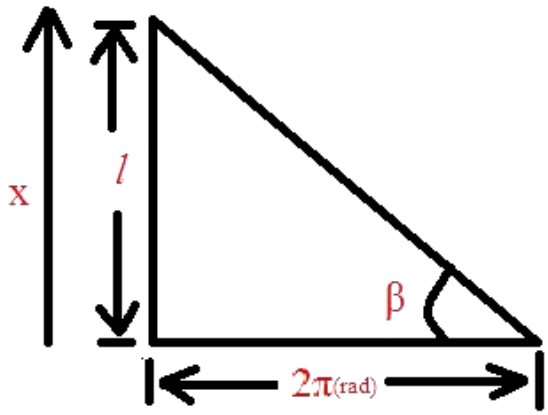

Fig. 7. Relation between angular and linear movement.

For six linear actuators above equation will be:

$$\sum_{i=1}^{6}\left(T_m(s)\right)_i = \sum_{i=1}^{6}\left((J_m s^2 + D_m s)\theta_m(s)\right)_i \tag{24}$$

We will solve here for one linear actuator.

Solving equations:

$$\frac{(R_a+L_a(s))(J_m s^2+D_m s)\theta_m(s)}{K_t} + K_b s\theta_m(s) = E_a(s) \tag{25}$$

Assuming that L_a is small as compared to R_a which is usual for a dc motor, so above equation becomes

$$\left[\frac{R_a}{K_t}(J_m s + D_m) + K_b\right] s\theta_m(s) = E_a(s) \tag{26}$$

Simplifying above equation yields,

$$\frac{\theta_m(s)}{E_a(s)} = \frac{K_t}{R_a J_m s^2+(R_a D_m+K_t K_b)} \tag{27}$$

Fig. 7 shows the relationship between the angular advance caused by the motor and the linear advance after the ball screw [19], in this case β represents the angle of the ball-screw lead; *l* represents the step of the lead and x(t) the linear advance [20].

$$x(t) = \frac{l}{2\pi}\theta_m(t) \tag{28}$$

Where$\theta_m(t)$ is given in radians and represents the angular advance generated by the motor.

So we have

$$\theta_m(t) = \frac{2\pi\, x(t)}{l} \tag{29}$$

And,

$$\frac{X(s)}{E_a(s)} = \frac{lK_t}{2\pi[R_a J_m s^2+(R_a D_m+K_t K_b)s]} \tag{30}$$

A free body diagram of the linear electric actuator is shown in Fig. 8 for a clarity.

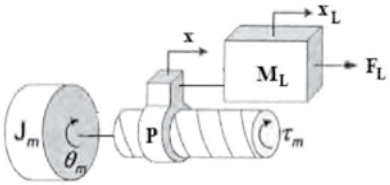

Fig. 8. Free body diagram of linear electrical actuator [18].

```
a = input('angle w.r.t x axis')
b = input('angle w.r.t y axis')
c = input('angle w.r.t z axis')
T = input('enter the coordinates')
r=4;%%upper platform radius
R=5.5;%%lower base radius
```

Fig. 9. Initial part of Matlab code to enter user defined data.

5. SIMULATION RESULTS

In this section simulation results are presented. These results include kinematic analysis, actuator's dynamics analysis and motion analysis of the bed.

5.1 Kinematic Analysis of the Bed

From the kinematics study done in section 3,a code was developed in MATLAB® for calculating lengths of actuators from known coordinates of the work piece. The initial data is entered by the user and code for it is as shown in Fig. 9. Using the initial data entered by the user and the equations (7) to (19) rotation matrix, B and P matrices are calculated. The code used for this purpose is given in Fig. 10. The final lengths of the legs are calculated using (5). The Matlab code of this is presented in Fig. 11.

In order to verify the inverse kinematic model of the machining bed, simulations were carried out on a work piece shown in Fig. 12. Four different positions of the work piece were selected as marked in Fig.12. The Matlab code calculated the desired lengths of all six legs for respective positions on the work piece. Results obtained from MATLAB® simulations are given in Table 2. In Table 2, **ϕ, Θ, Φ** are rotations about X, Y and Z axis respectively whereas L1, L2, L3, L4, L5, L6 are lengths of linear actuators. All the lengths and coordinates are in mm.

```
PRB=[cos(b)*cos(a) -sin(b)*cos(c)+cos(b)*sin(a)*sin(c)sin(b)*sin(c)+cos(b)*sin(a)*cos(c);
    sin(b)*cos(a) cos(b)*cos(c)+sin(b)*sin(a)*sin(c) -cos(b)*sin(c)+sin(b)*sin(a)*cos(c);
    -sin(a) cos(a)*sin(c) cos(a)*cos(c)]

b1=[R*cos(12.5);R*sin(12.5);0];
b2=[R*cos(47.5);R*sin(47.5);0];
b3=[R*cos(47.5);R*sin(47.5);0];
b4=[-R*cos(12.5);R*sin(12.5);0];
b5=[-R*cos(17.5);-R*sin(17.5);0];
b6=[R*cos(17.5);-R*sin(17.5);0];

p1=[r;0;0];
p2=[-r*cos(60);r*sin(60);0];
p3=[-r*cos(60);r*sin(60);0];
p4=[-r;0;0];
p5=[-r*cos(60);-r*sin(60);0];
p6=[r*cos(60);-r*sin(60);0];
```

Fig. 10. Middlepart of Matlab code to calculate matrices from user defined data.

```
L1 = T+PRB *p1-b1;
length1 = norm(C1);
L2 = T+PRB *p2-b2;
length2 = norm(C2);
L3 = T+PRB *p3-b3;
length3 = norm(C3);
L4 = T+PRB *p4-b4;
length4 = norm(C4);
L5 = T+PRB *p5-b5;
length5 = norm(C5);
L6 = T+PRB *p6-b6;
length6 = norm(C6);
```

Fig. 11. Part of Matlab code calculating lengths of six legs required to move to the desired positions.

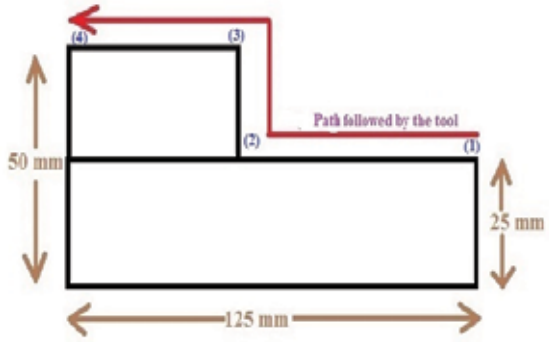

Fig. 12. Work piece used for machining.

Table 2. Length of linear actuators calculated for different coordinates.

Φ (deg)	Θ (deg)	Φ (deg)	Coordinates (mm)	L_1 (mm)	L_2 (mm)	L_3 (mm)	L_4 (mm)	L_5 (mm)	L_6 (mm)
0	0	0	0,0,430	53	74	74	53	60	60
0	0	0	0,75,430	54	77	77	54	60	60
0	0	0	0,75,450	74	96	96	74	79	79
0	0	0	0,125,450	81	105	105	81	85	85

5.2 Dynamics Analysis of Linear Actuator

In order to verify the dynamics of the linear actuators an open loop model was created in Simulink, a tool box of Matlab, where the transfer function of the motor was implemented. Substituting values of constants in (30) following transfer function is obtained and this is embedded in the Simulink model:

```
Transfer function:
                0.0015
---------------------------------
0.000338 s^3 + 42.48 s^2 + 0.045 s
```

To verify the dynamics of the motor, a step response of the open loop system was observed as shown in Fig. 13-a. On the graph time in seconds is on horizontal axis and Amplitude of the displacement is on vertical axis. From open loop response it was expected that the length of linear actuator increases with increase in applied voltage and this behaviour can be seen in Fig. 13-a.The length of linear actuator is increasing linearly but approaching to infinity as time approaches to infinity but the system requirement is to achieve a desired length.

In order to achieve the desired length the system needs to be closed loop. A proportional controller is designed, therefore, and tuned. As a result of auto tuning a proportional gain of 43 is chosen which gives rise time 0.395 seconds and settling time 0.676 seconds with no overshoot. A response of the closed loop system is shown in Fig. 13-b. The closed loop system is now stable and each motor generates the desired input to the lead screws of the linear actuators to give desired lengths of legs within half a second without overshoot of the top plate of the machining bed. More benefits of closed loop response are that precise

results are obtained, error is minimized and information about the position of end effect or may be obtained.

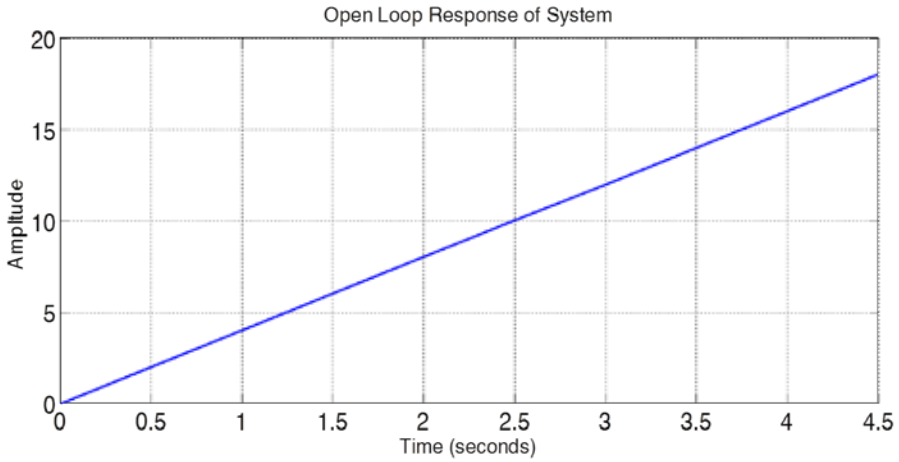

Fig. 13-a. Open loop response of the actuator of machining bed system.

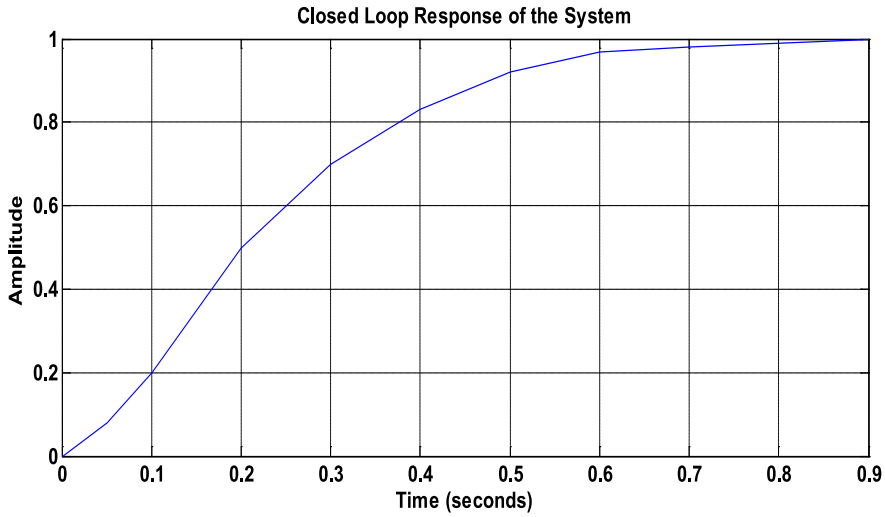

Fig. 13-b. Closed loop response of the actuator of machining bed system.

5.3 Motion Analysis of Bed

For simulations of motion of the proposed six degree of freedom machining bed software called Solid work® was used. The leg lengths were assumed to be same (380 mm: distance between bottom and top plates when the linear actuators are closed) initially. Simulation was performed in Solid Works and movement of bed was tested for 6 degree of freedom by giving different lengths to linear actuators. Fig. 14-a and14-b show shots of the movement of bed with different actuator leg length. The motion presented in Fig. 14-a was generated in x-axis only while Fig. 14-b is generated in three dimensions. The movements were observed as per expectations which verify that the design is acceptable for a parallel manipulator to be used as a 6 DOF machining bed. The leg lengths calculated in section 5.1 for the work piece shown in Fig. 12 were used to simulate motion of the machining bed in Solid Works. The resulting values of position of the centre of top plate and the position values (reference values) for which leg

lengths were calculated are plotted for two different cases of motion as shown in the Fig. 15a and Fig. 15b. The difference in plots is error in position. This error occurred due to losses in lead screw or friction in the joints and may be removed in future using position feedback and a controller to make the overall system as closed loop system.

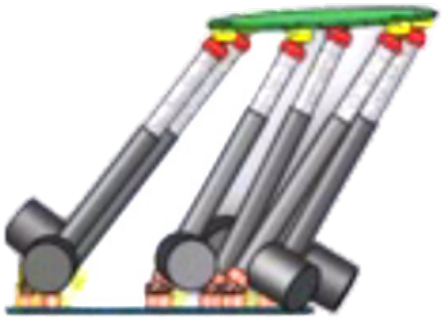

Fig. 14-a. Motion of top plate of machining bed in x-axis.

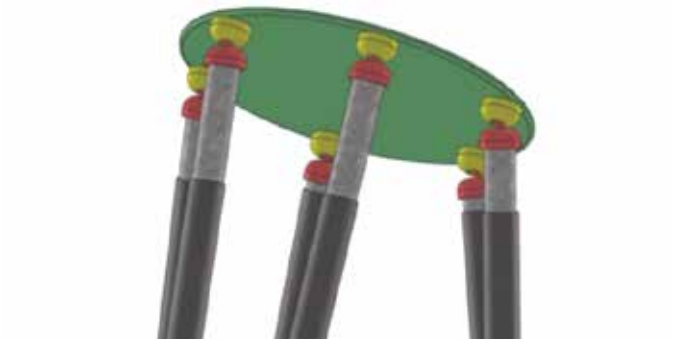

Fig. 14-b. Motion of top plate of machining bed in three axes.

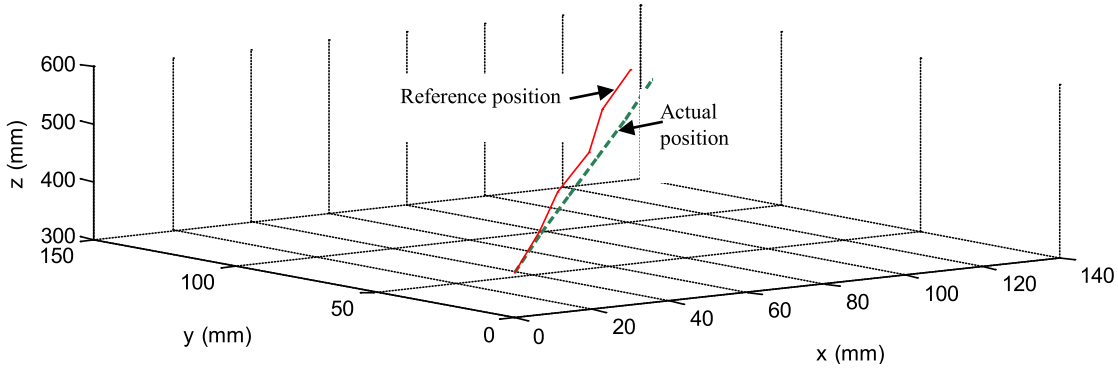

Fig. 15-a. Reference and actual positions of centre of top plate of the machining bed when variation is in x, y & z axis.

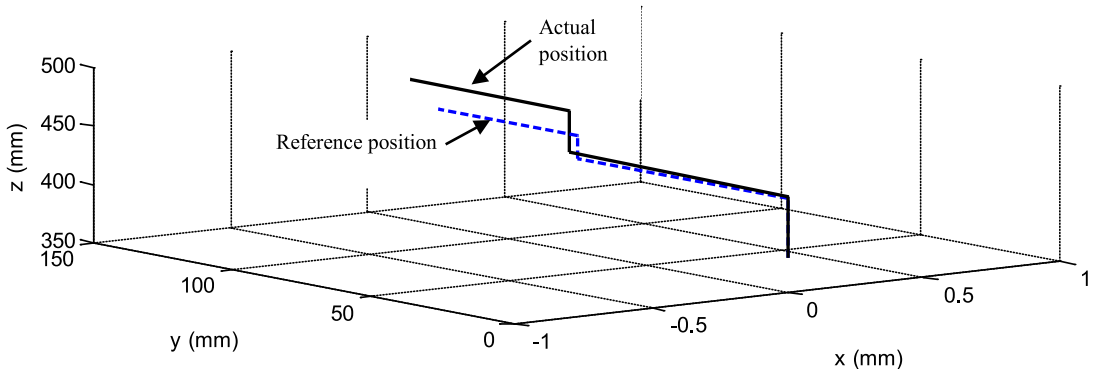

Fig. 16-b. Reference and actual positions of centre of top plate of the machining bed when variation is in y and z axis only.

6 CONCLUSIONS

We have presented a design for a parallel robotic mechanism for a machining bed, the inverse kinematics of the parallel robot and dynamics model of linear actuator. We used Solid Works to simulate the behaviour of the design of bed, dynamics model for linear actuator was verified using MATLAB® and kinematic study for the platform is used to find the lengths of linear actuator for different coordinates in MATLAB®. It is concluded that the use of a 6 DOF parallel mechanism as a machining bed provides the desired results and the verified model of the proposed mechanism may be used for the bed control design and the development of the bed for machining. A control design and implementation will produce precision and accuracy.

7. REFRENCES

1. Sutherland, J.W. *Lecture Notes on Manufacturing*. *Department of Mechanical Engineering, Michigan Technological University,* Houghton, MI, USA. www.mfg.mtu.edu/cyberman/machining.html (Accessed on March 03, 2015).
2. Kausar, Z. M., A. Irshad & S. Shahid. A parallel robotic mechanism replacing a machine bed for micro-machining. In: *Scientific Cooperations International Workshops on Electrical and Computer EngineeringSubfields,* 22-23 August 2014, Istanbul, Turkey, p. 228-233 (2014).
3. Stewart, D. A platform with six degrees of freedom. *Proceedings of Institution of Mechanical Engineers* 180(1): 371–386 (1965).
4. Lee, S. H., J.B. Song, W.C. Choi & D. Hong. Position control of a Stewart platform using inverse dynamics control with approximate dynamics. *Mechatronics* 13(6): 605–619(2003).
5. Liu, K., J. Fitzgerald, & F.L. Lewis. Kinematic analysis of a Stewart platform manipulator. *IEEE Transactions of Industrial Electronics* 40(2):282–93 (1993).
6. Lebret, G., K. Liu, & F.L. Lewis. Dynamic analysis and control of a Stewart platform manipulator. *Journal of Robotic Systems* 10(5):629–655 (1993).
7. Dasgupta, B, & T.S. Mruthyunjaya. Closed-form dynamic equations of the general Stewart platform through the Newton–Euler approach. *Mechanism and Machine Theory* 33(7):993–1012 (1998).
8. Zhang, C., & S. Song. An efficient method for inverse dynamics of manipulators based on the virtual work principle. *Journal of Robotic Systems* 10(5):605–627 (1993).
9. Fichter, E.F.A Stewart platform-based manipulator: general theory and practical construction. *International Journal of Robotics Research* 5(2):157–182 (1986).
10. Zhiming, J. Study of the effect of leg inertia in Stewart platforms. In: *International Conference on Robotics and Automation*, p. 121–126 (1993).
11. Wang, Y. *Symbolic Kinematics and Dynamics Analysis and Control of a General Stewart Parallel Manipulator*. MS thesis, Department of Mechanical and Aerospace Engineering, State University of New York, Buffalo, New York, USA (2008).
12. Valenti, M. Machine tools get smarter. *ASME Mechanical Engineering* 117(11): 70–75 (1995).

13. Kim, J.W., et al. Performance analysis of parallel manipulator architectures for CNC machining. In: *Proc. ASME International Mechanical Engineering Congress and Exposition Symposium on Machine Tools*, Dallas, TX, USA (1997).
14. Dwarakanath, T.A., B. Dasgupta & T.S. Mruthyunjaya. Design and Development of a Stewart platform based Force-Torque Sensor. *Mechatronics* 11(7): 793-809 (2001).
15. Zaiter, A.A., E.L. Ng, S. Kazi & M.S.M. Ali**.** Development of Miniature Stewart Platform Using TiNiCu Shape-Memory-Alloy Actuators. *Advances in Materials Science and Engineering*, Vol. 2015, 928139, (2015).
16. Wulfsberg, J.P, T. Redlich, & P. Kohrs. Square foot manufacturing: a new production concept for micro manufacturing. *Production Engineering* 4(1): 75–83 (2010).
17. Bingul, Z., & O. Karahan. Dynamic Modeling and Simulation of Stewart Platform. In: *Serial and Parallel Robot Manipulators-Kinematic, Dynamics, Control and Optimization.* INTECH, Croatia, p. 19-44 (2012).
18. Norman, S.N. *Control Systems Engineering*. John Wiley & Sons, p. 79-85 (1995).
19. Ruiz-Rojas, E.D., J.L. Vazquez-Gonzalez, et.al. Mathematical Model of a Linear Electric Actuator with Prosthesis Applications. In: IEEE *International Conference on Electronics, Communications and Computers* 3-5 March, Puebla, p.182 - 186(2008).
20. Kim, M.S., & S.C. Chung. A systematic approach to design high-performance feed drive system. *International Journal of Machine Tools & Manufacture* 45(12-13): 1421-1435 (2005).